

MEASURING CORRELATIONS BETWEEN BEAM LOSS AND RESIDUAL RADIATION IN THE FERMILAB MAIN INJECTOR*

Bruce C. Brown, Guan Hong Wu, Fermilab, Batavia, IL 60510, USA

Abstract

In order to control beam loss for high intensity operation of the Fermilab Main Injector, electronics has been implemented to provide detailed loss measurements using gas-filled ionization monitors. Software to enhance routine operation and studies has been developed and losses are logged for each acceleration cycle. A systematic study of residual radiation at selected locations in the accelerator tunnel have been carried out by logging residual radiation at each of 142 bar-coded locations. We report on fits of the residual radiation measurements to half-life weighted sums of the beam loss data using a few characteristic lifetimes. The data are now available over a multi-year period including residual radiation measurements repeated multiple times during three extended facility shutdown periods. Measurement intervals of a few weeks combined with variable delays between beam off time and the residual measurement permits sensitivity to lifetimes from hours to years. The results allow planning for work in radiation areas to be based on calibrated analytic models.

BASIC RELATIONSHIPS

The orbits used in Main Injector operation are quite stable. Most beam loss is at or near the injection energy of 8 GeV. Losses are dominated by the uncaptured beam loss from slip stack injection, beam in kicker gaps and 8 GeV beam lifetime issues. Variations are frequently due to small changes in the Booster beam quality. As a result, we will assume that the local geometry and energy of losses are always the same. Improvements in removal of beam from kicker gaps by anti-damping and improved collimation is responsible for the long term trends. With this assumption, the relation between Beam Loss Monitor (BLM) readings and residual radiation in the tunnel is fixed. We will explore our ability to correlate one BLM reading and residual radiation at some nearby point.

We illustrate this argument using Fig. 1 where we see a simulation of the residual radiation from beam loss in the collimation region of the Main Injector. Lost beam which was scattered by the primary collimator upstream is mostly captured in the secondary collimators but beam is also lost in other devices. The radiation fields for prompt radiation, residual radiation and absorbed dose are very similar.

The basis for linearly relating loss and residual radiation lies in the following arguments:

1. For a fixed loss pattern (as assumed), the prompt radiation field produced by losses will produce a distribution of isotopes in the devices near the beam. The number of radioactive nuclei will be proportional to the beam lost.

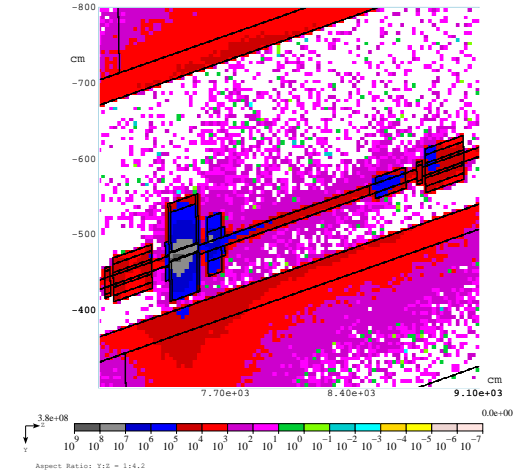


Figure 1: MARS simulation of loss region near Main Injector secondary collimator.

tion of isotopes in the devices near the beam. The number of radioactive nuclei will be proportional to the beam lost.

2. This radiation field will also produce ionization in nearby Beam Loss Monitors (BLM's) and the ionization signal will also be proportional to the number of lost protons.
3. The radioactive nuclei will emit radiation including gamma rays which can be detected by the Geiger counter used to monitor residual radiation. At each monitor point, the efficiency with which the Geiger counter records signals due to the spatial pattern of isotopes and the spectra of the radioactive decays is dependent only on the isotope being detected.

MEASUREMENTS

Residual Radiation Data

In preparation for higher intensity operation for the Main Injector neutrino program (NuMI), residual radiation measurements were undertaken beginning in 2004 to identify loss issues. Locations of interest were identified. A radiation meter was purchased with two internal Geiger tubes (for measurements from 50 micro-Roentgen/hr to 100 Roentgen/hr), a bar code reader to identify monitoring locations and memory to store results. Bar coded tags were installed. Measurements with this system have been carried out as access time permitted since 10 October 2005[1]. For some accesses, the delay between beam loss and residual radiation measurement was a couple of hours. Intermediate

* Operated by Fermi Research Alliance, LLC under Contract No. DE-AC02-07CH11359 with the United States Department of Energy.

cases involved delays of 12 to 36 hours. Maintenance and upgrade shutdowns of the Fermilab facility have allowed a series of measurement without addition loss of up to 90 days.

Beam Loss Monitor Data

Real time beam loss monitoring is accomplished in the Main Injector using the argon gas ionization detector described in [2]. BLM's are placed a bit above the beam line height against the tunnel outer wall at the downstream end of each quadrupole. Monitors are placed along the extraction channels more densely to monitor losses at the transfer points. A current, proportional to the ionization which the beam loss creates, is delivered to the BLM electronics. The BLM electronics integrates the charge in 22 microsecond intervals and accumulates various sliding sums to be reported or to be used for beam aborts. For this work we employ the sums accumulated for and read out at the end of each Main Injector acceleration cycle. Using the well-documented calibration of these devices, the results are stored and reported in Rads[3].

ANALYSIS FORMULAS

We wish to employ these tools to provide detailed predictions of radiation to be expected during access to locations near the monitor locations. For this purpose we will devise decay curves based on a few isotopes. The data is unable to constrain a richer model and for the modest precision required, representation by three or four dominant isotopes is sufficient. The delays required for safe access limit the interesting isotopes to ones with half life greater than many minutes.

To prepare for this analysis, we sum the BLM integral for each Main Injector cycle into 'quanta', LI_j .

$$LI_j = \sum_{t=t_j}^{t_j+T_s} LI(t) \quad (1)$$

taking $T_s = 600$ sec. The loss rate is given by $LR_j = LI_j/T_s$, where LI_j is in Rads and LR_j is in Rads/sec. Using these 'quanta', we compute exponentially weighted sums, LW , weighting by the half-life of interest. Rates will be more convenient, thus we normalize appropriately.

$$LW(I, T_M) = \sum_j LI_j \times \frac{\ln 2}{\tau_I} 2^{-(T_M - T_j)/\tau_I} \quad (2)$$

where T_M is the residual radiation measurement time, T_j is the quanta time and τ_I is the half life for isotope I . With times in seconds, LW is in units of Rads/sec.

With our assumptions above, the residual radiation $RR(T_M)$ at a monitor point is related to the weighted sum of the losses at a nearby BLM, $LW(I, T_M)$ using a single coefficient E_I for each isotope of interest

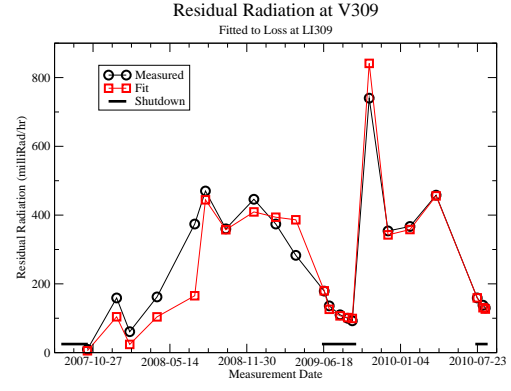


Figure 2: Residual radiation and results of fitting to weighted loss rates for measurements at trim dipole V309, downstream of the fourth secondary collimator. Loss rates at LM309 are summed to provide LW . Half lives of 312.3 days, 5.591 days and 2.58 hours are used in this fit.

$$RR(T_M) = \sum_I E_I \times LW(I, T_M) \quad (3)$$

Note that all of the geometric factors for the loss distribution, the production of BLM ionization by the shower, the production of isotopes, the geometric sensitivity and energy response of the Geiger tube can all be multiplied together into the single linear coefficient per isotope, E_I . This system of equations can be solved by matrix inversion to provide values for E_I .

In Fig. 2, we have applied this to data in the MI collimator region where we added bar code locations during the collimator installation. Radiation in this region was low before the collimator installation. At other locations, significant residual radiation was present prior to the commissioning of the BLM electronics. Long-lived residual radiation was important in these regions as the BLM monitoring began. For this situation, we note that the time between residual radiation monitoring tours is typically long compared to all but the longest isotope half life. With that in mind, we add a term to the above equation in which a fraction f of the observed measurement $RR(T_R)$ is due to this isotope.

$$RR(T_M) = \sum_I E_I \times LW(I, T_M) + f \times RR(T_R) 2^{-(T_M - T_R)/\tau_L} \quad (4)$$

We are still able to fit using matrix inversion to obtain f in addition to the E_I . In Fig. 3 we show fits with and without the inclusion of residual radiation data from the period before the logging of BLM data. The data is at a monitoring point at the upstream end of the Lambertson magnet used for extraction to the anti-proton target, the Tevatron and external beams. The decay of long lived isotopes is satisfactorily described by this fit.

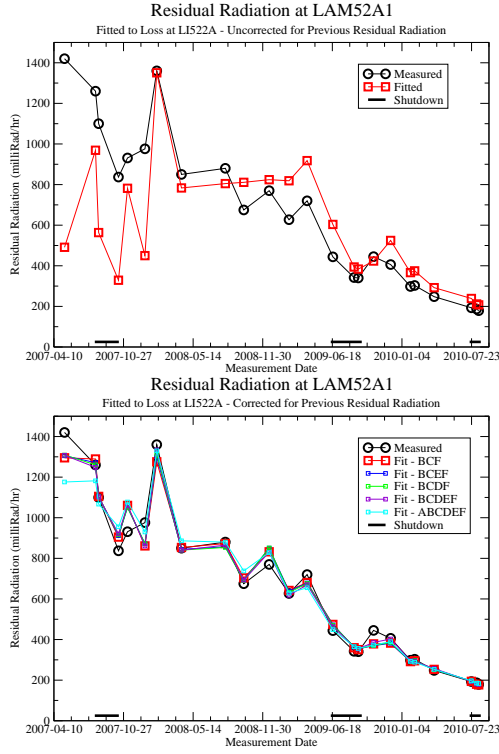


Figure 3: Fits of the measured residual radiation at a location on the primary extraction Lambertson magnet, LAM52A2 without (above) and with (below) the correction for radiation prior to the BLM data record.

In Table 1, we show half lives used for fitting along with an isotope of that half life. Some may be the important isotope produced whereas other may only represent a half life in the appropriate range. In Table 2, we list the values of E_I from a fit to the residual radiation near the upstream vacuum pump on the first extraction Lambertson at MI52. Fits using matrix inversion are not constrained to provide positive coefficients so we see unphysical values for some table entries. However, we see in Fig. 3 that the curves are quite similar for the various fits.

PREDICTING RADIATION: V401

The 2010 shutdown work included electrical work to connect cables for kicker magnets which will direct beam which slipped into the gap for the injection kickers (gap

Table 1: Isotopes in Fit for LAM521A1

label	Isotope	Halflife
A	^{22}Na	2.6 years
B	^{54}Mn	312.3 days
C	^{52}Mn	5.591 days
D	^{24}Na	15 hours
E	^{52}Fe	8.275 hours
F	^{56}Mn	2.58 hours

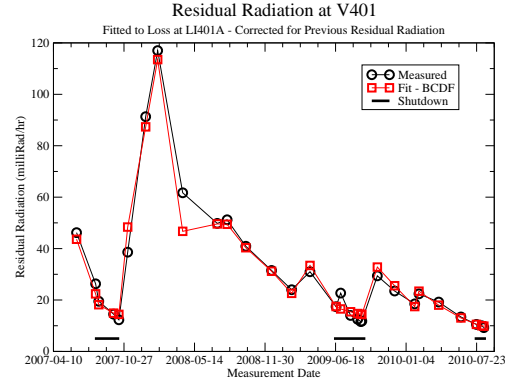


Figure 4: Residual radiation and results of fitting to weighted loss rates for measurements at trim dipole V401, downstream of the abort kicker. Loss rates at LM401A are summed to provide LW . Half lives of 312.3 days, 5.591 days, 15 hours and 2.58 hours are used in this fit.

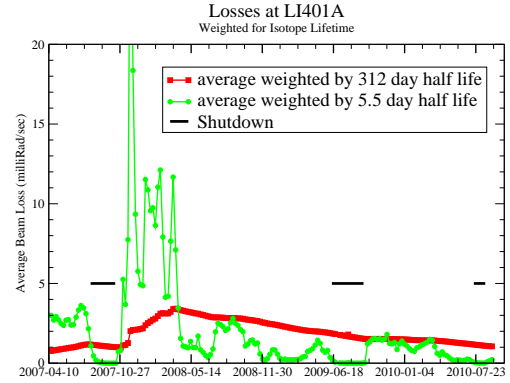


Figure 5: Exponential weighted losses, LW , measured by LM401A are shown for half lives of 312 days and 5.5 days.

clearing kickers). This involved extensive time for work between the kickers in MI400 and the abort Lambertson magnets at MI402. Following the 2009 shutdown, monitoring of this area was a priority. When it was noted that residual radiation was higher than expected, collimator vertical positions were modified to permit the anti-damping system to drive the unwanted beam into the collimators rather than the kicker apertures between MI400 and MI401. Fig. 4 shows the measured and fitted loss patterns. Weighted loss data used in that fit are shown in Fig. 5. This study per-

Table 2: Fit coefficients, E_I ($\times 10,000$) for various isotope combinations used to fit data on residual radiation at LAM52A1

A	B	C	D	E	F
-1.0585	0.3709	0.1210	0.2857	-0.3872	0.4640
	0.2494	0.1446	0.3360	-0.4837	0.6708
	0.2480	0.1948			0.3929
	0.2523	0.1741		0.1053	0.1620
	0.2528	0.1611	0.0779		0.2116

mitted planning for the work while assuring low enough radiation exposure to the workers.

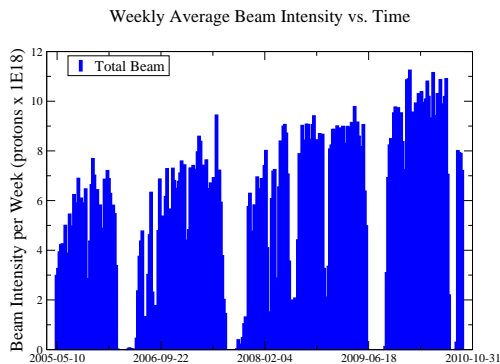


Figure 6: Protons delivered by the Main Injector for production of anti-protons and neutrinos in the NuMI Era.

LOSS AND RESIDUAL RADIATION HISTORY

In Fig. 6 and Fig. 7 we document the progress achieved in loss control in the Main Injector. In Fig. 6 we see that following the commencement of the Neutrinos at the Main Injector (NuMI) beam operation, fluxes of 6×10^{18} were achieved in a few months. Addition of 11-batch slip stacking injection allowed intensities for the anti-proton and neutrino beam combined of more than 10×10^{18} per week. In Fig. 7 we show the results of seven of the more than 40 residual radiation measurement tours around the Main Injector tunnel. We see that the steady decrease in residual radiation shown in Fig. 3 is repeated around much of the ring. Additional tools are being applied to allow further reduction in the number of points where losses are significant.

CONCLUSIONS AND ISSUES

The goal of providing residual radiation predictions for planning work on the Main Injector has been met by this simple analysis. Predicted radiation decay curves will be adequate for exposure planning. We note, however, that the fits are not ‘good fits’ as measured by χ^2 and the fit using matrix inversion will produce unphysical (negative) coefficients for some data sets. Detailed decay measurements at a few locations can provide constraints on the actual half life components of interest. Simulations of the radiation using MARS will be employed to try to match predicted isotopes and observed half life measurements.

ACKNOWLEDGMENTS

We would like to thank the Accelerator Division Instrumentation Group and the Controls Group for their support of the Beam Loss Monitor data acquisition system and the data logging of the results. Special thanks to Marvin Olson, Randy Thurman-Keup and Charles Briegel.

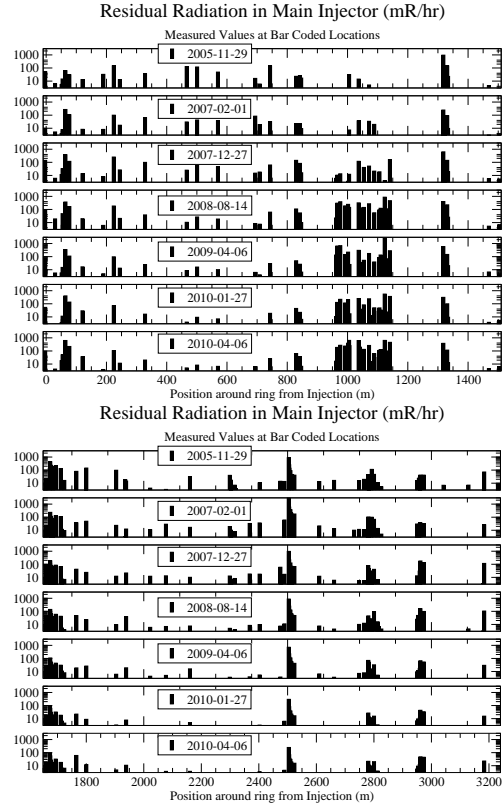


Figure 7: Residual Radiation at the monitor points around the Main Injector. Upper plot from Injection to the Abort. Lower plot from the abort to the injection region. Residual radiation levels have grown at the collimator region (1000 m). Lambertson magnets at MI400 (Abort - 1700 m), MI52 (Multi-extraction point - 2500 m), MI608 (NuMI Extraction - 2780 m) and MI62 (PBar Transfer - 2950 m) mostly show substantial to dramatic reductions in radiation levels. Some other locations have had residual radiation drop to insignificant levels. Note that this is a three decade log plot from 3 to 3000 mR/hr.

REFERENCES

- [1] Bruce C. Brown. Residual Radiation Monitoring in the Main Injector with the ROTEM RAM DA3-2000 Radiation Survey Meter. Beams-doc 3523 v1, Fermilab, December 2009.
- [2] R.E. Shafer, R.E. Gerig, A.E. Baumbaugh, and C.R. Wegner. The Tevatron Beam Position and Beam Loss Monitoring Systems. In Francis T. Cole and Rene Donaldson, editors, *Proceedings of the 12th International Conference On High-Energy Accelerators*, pages 609–615. Fermilab, 1983. Also available as FERMILAB-CONF-83-112-E.
- [3] Bruce C. Brown and Guan H. Wu. Some Console Applications for Displaying Main Injector BLM Measurements. Beams-doc 3299 v2, Fermilab, June 2009.